European Polymer Journal 96 (2017) 248–255

Contents lists available at ScienceDirect

European Polymer Journal

journal homepage: www.elsevier.com/locate/europolj

High molecular weight poly(butylene succinate-co-furandicarboxylate) with 10 mol% of BF unit: Synthesis, crystallization-melting behavior and mechanical properties

Shuangbao Peng[a], Zhiyang Bu[a], Linbo Wu[a,*], Bo-Geng Li[a], Philippe Dubois[b,c,*]

[a] State Key Laboratory of Chemical Engineering at ZJU, College of Chemical and Biological Engineering, Zhejiang University, Hangzhou 310027, China

[b] Laboratory of Polymeric and Composite Materials (LPCM), Center of Innovation and Research in Materials and Polymers (CIRMAP), University of Mons, Mons 7000, Belgium

[c] Materials Research and Technology Department (MRT), Luxembourg Institute of Science and Technology (LIST), Esch-sur-Alzette 4362, Luxembourg

ARTICLE INFO

Keywords:
Biobased polymers
Biodegradable polymers
Copolyesters
2,5-Furandicarboxylic acid
Crystallization
Crystal structure
Mechanical properties

ABSTRACT

In this study, high molecular weight poly(butylene succinate-co-furandicarboxylate) with 10 mol % of butylene furandicarboxylate unit (PBSF10) was synthesized and its crystal structure and crystallization-melting behaviors were investigated by means of WAXD, SAXS, DSC and POM. The tensile properties were also assessed. The crystal structure of PBSF10 is found to be the same as that of poly(butylene succinate) (PBS). The SAXS result indicates that PBSF10 had the same thicknesses of crystalline region and transition zone, but larger thickness of amorphous region, indicating that the BF units are mostly excluded from the crystalline region and located in the amorphous region. Therefore, PBSF10 is less crystallizable than PBS. But PBSF10 still exhibits rapid nonisothermal and isothermal crystallization. Because of high molecular weight and good crystallizability, PBSF10 exhibits superior tensile properties: modulus 370 MPa, strength at break 38 MPa and elongation at break 230%.

1. Introduction

Biobased and biodegradable polymers are deemed as green and sustainable materials from cradle to grave. Manufacturing and using biobased and biodegradable polymers instead of some non-degradable ones has been proved to be an effective way to realize the carbon-neutral circle [1,2] and to solve, at least partially, the white pollution problem resulted from discarded polymeric materials [3]. Poly(lactic acid) (PLA) [4,5] and poly(butylene adipate-co-terephthalate) (PBAT) [6–9] are the most representative rigid and flexible biodegradable polymers, respectively. They have been successfully commercialized and extensively used into a variety of fields from disposable daily necessities to mulch films. PLA is a biobased polymer but PBAT is not yet. As 2,5-furandicarboxylic acid (FDCA) emerged as a new biobased aromatic monomer in the recent decade [10,11], some new biobased aliphatic-aromatic flexible copolyesters [12–20], including poly(butylene succinate-co-furandicarboxylate) (PBSF) [12,13,16,17] and poly(butylene adipate-co-furandicarboxylate) (PBAF) [14–17], emerged as biodegradable polymers.

Synthesis, thermo-mechanical properties, hydrolytic and biological degradation of FDCA-based copolyesters have been reported in recent years [12–20]. As FDCA has similar molecular structure as that of terephthalic acid (TPA) [11], these biobased copolyesters

* Corresponding authors at: College of Chemical and Biological Engineering, Zhejiang University, Zheda Rd 38, Hangzhou 310027, China (L. Wu). Center of Innovation and Research in Materials and Polymers (CIRMAP), University of Mons, Mons 7000, Belgium, (P. Dubois).

E-mail addresses: wulinbo@zju.edu.cn (L. Wu), philippe.dubois@umons.ac.be (P. Dubois).

http://dx.doi.org/10.1016/j.eurpolymj.2017.09.008
Received 6 May 2017; Received in revised form 19 August 2017; Accepted 7 September 2017
Available online 09 September 2017
0014-3057/ © 2017 Elsevier Ltd. All rights reserved.

display thermo-mechanical properties comparable to the TPA-based counterparts [6–9,21–25]. It was reported that PBAFs with an butylene furandicarboxylate (BF) unit content below 50% are enzymatically degradable in the presence of lipase from porcine pancreas [14] and PBSFs with BF content less than 20% possess good compost biodegradability as well [13]. Our previous study demonstrated the hydrolytic [16] and compost [17] degradation of PBSFs and PBAFs with 40–60 mol% BF unit. Therefore, PBAF and PBSF copolyesters appear to be promising biobased and biodegradable polymers with attractive performance and potentially wide applications.

In general, thermo-mechanical properties of aliphatic-aromatic copolyesters are strongly composition-dependent [8,12,15,16,21,22]. Usually, copolyesters containing around 50 mol% aromatic unit exhibit good biodegradability and better comprehensive thermo-mechanical properties. For an example, the commercialized PBAT copolyesters often contain about 45% butylene terephthalate (BT) unit. However, such copolyesters with "middle" composition are often less crystallizable than the aliphatic- or aromatic-rich copolyesters [8,12,15,21,22]. In our previous studies, we reported the synthesis and composition-dependent thermo-mechanical properties of PBSF [12] and PBAF [15] in the whole composition range. These copolyesters are less crystallizable at 40–60% BF but have good crystallizability at 10% BF. It is well-known that poly(butylene succinate-co-adipate) (PBSA) copolyesters with 10–20% BA unit are deemed as chemically modified PBS products [26,27] and have been commercialized together with PBS. Similarly, PBSF copolyesters with BS-rich composition may also find practical applications as modified PBS thank to good crystallizability [12], compost degradability [13] and tunable property, and therefore deserve more attention and research to better understand the structure-property relationship of these FDCA-based copolyesters.

As one of a series of study on PBSF/PBAF copolyesters [12,15–17], in this study, we report the synthesis, crystal structure, crystallization kinetics, melting behavior and mechanical properties of high molecular weight PBSF containing 10% BF unit (PBSF10) and PBS. The crystal structure was studied with WAXD and SAXS. The nonisothermal and isothermal crystallization and melting behaviors were investigated with DSC. And the spherulite growth was investigated with POM and analyzed with Lauritzen-Hoffman equation. The tensile properties were also assessed.

2. Experimental

2.1. Materials

Succinic acid (SA, Anhui Sanxin Chem. Co., China), 1,4-butanediol (BDO, Sinopec Yizheng Chem. Fibre Co., China) and tetrabutyl titanate (TBT, ≥99.0%, Aladdin) were all used as received. Highly purified 2,5-furandicarboxylic acid (FDCA) purified with our previously reported method [15] was supplied by Satar Chem. Co., China. Some possible impurities like 5-formyl-2-furancarboxylic acid and acetic acid were completely undetectable in its ^{1}H NMR spectrum (not shown here).

2.2. Synthesis

PBS and PBSF10 were synthesized from BDO, SA and FDCA (optional, 10 mol% in diacid) via a two-step melt polycondensation procedure. In brief, the monomers (diol/diacid molar ratio 2:1) were added into a 250 mL four-necked round flask under mechanical stirring and N_2 inlet and then heated to 170 °C. TBT (0.1 mol% based on diacid) was added and the esterification reaction was conducted at 170 °C for 1 h, 180 °C for 2 h and 190 °C for 1–2 h up to over 98% esterification degree. Finally, the polycondensation reaction was performed under vacuum (< 240 Pa) at 230 °C for 1 h and 240 °C for 2–5 h until Weissenberg effect emerged. The products were vacuum-dried at 40 °C for more than 24 h and stored in a desiccator before characterization and testing.

2.3. Characterization

The ^{1}H NMR spectrum was recorded with an AC-80 spectroscopy (400 MHz, BRUKER). Deuterated chloroform was used as solvent and tetramethylsilane as internal reference. δ_H ($CDCl_3$): 4.11 (4H, t), 2.63 (4H, s), 1.71 (4H, m) for PBS; 7.21 (2H, d), 4.40 (4H, t), 4.36 (2H, t), 4.15 (2H, t), 4.11 (4H, t), 2.63 (4H, s), 1.92 (4H, m), 1.85 (2H, m), 1.77 (2H, m), 1.71 (4H, m) for PBSF.

The molecular weight and its distribution were measured at 30 °C by a gel permeation chromatography (GPC, Waters 1525/2414) equipped with a differential refractive index detector (DRI, Water 2414). Chloroform was used as eluent. The concentration of sample solution was about 3 mg/mL, and the eluent flow rate was 1.0 mL/min. Polystyrene standards were used for calibration. The intrinsic viscosity was measured at 25 °C by an automatic viscosity tester (ZONWON IVS300, China) equipped with a Ubbelohde viscometer with a diameter of 0.88 mm. Mixture of phenol and tetrachloroethane (3/2 w/w) was used as solvent. The solution concentration was 5 mg/mL. The intrinsic viscosity was calculated via Billmeyer empirical formula $[\eta] = (\eta_{sp} + 3\ln\eta_r)/4$ C [28].

The wide angle X-ray diffraction (WAXD) pattern was recorded using a X'Pert Pro X-ray diffraction system (PANalytical B.V. Company, Netherland) with Cu Kα radiation (1.54 Å), working at 40 KV and 200 mA. The sample was scanned from $2\theta = 5^\circ$ to $2\theta = 60^\circ$ with scanning rate of 2°/min. The small angle X-ray scattering pattern was recorded using XEUSS SAX. S system (XENOCS SA, France) with CuKα radiation (1.54 Å), working at 40 KV and 200 mA. The sample was scanned from $2\theta = 0.1^\circ$ to $2\theta = 3.6^\circ$ with scanning rate of 0.05°/min.

The thermal transition was recorded with differential scanning calorimetry (DSC) on a Q200 thermal analyzer (TA Instruments). A standard heat-cool-heat program with heating/cooling rate of 10 °C/min was performed between −50 and 150 °C. The temperature was held at 150 °C and −50 °C for 5 min respectively before cooling and second heating. For isothermal melt crystallization and melting, a sample was heated to 150 °C and kept for 5 min, then cooled rapidly to the crystallization temperature and held at this

Table 1
Chain structure parameters of PBS and PBSF10.

Sample	M_w (g/mol)	$Đ$	$[\eta]$[a] (dL/g)	ϕ_{BF} (mol%)	Ref.
PBS	162,500	1.93	1.37	0	This study
PBSF10	193,700	2.32	1.91	10.2	This study
PBS*	35,100	1.71	–	0	[12]
PBSF10*	55,800	2.52	–	9.72	[12]

[a] The intrinsic viscosity was measured at 25 °C in phenol/tetrachloroethane (3/2 w/w) solvent.

temperature for enough time (10–85 min) in order to crystallize completely. At last, it was re-heated to 150 °C at 10 °C/min.

Spherulite growth was observed with a polarized optical microscope (POM, ECLIPSE E600W POL). The sample was heated at 10 °C/min to 150 °C and held for 3 min, then rapidly cooled at −100 °C/min to the crystallization temperature (T_c) and crystallized at T_c for enough time to observe and record the growth of spherulite.

The tensile properties were measured with a Zwick Roell Z020 testing machine according to ASTM D638. Dumbbell-shaped tensile specimens with thickness of 2 mm were prepared by injection with a HAAKE MiniJet II injector. All the specimens were kept in standard atmosphere of 25 °C and 50% relative humidity for at least 48 h before testing. The crosshead speed was 10 mm/min. For each sample, at least five specimens were tested in parallel.

3. Results and discussion

3.1. Synthesis and chain structure

PBS and PBSF10 were synthesized via a two-step melt polycondensation procedure. The intrinsic viscosities of them were of 1.37 dL/g and 1.91 dL/g, respectivley. And the weight average molecular weights of them were of 162,500 and 193,700 g/mol, respectivley. The molecular weights were much higher than those reported in our previous study [12] (see Table 1) because much purer FDCA monomer and optimized reaction conditions were used in this study. The lower and escalating esterification temperature program was helpful to depress the etherification side reaction and therefore to reach high esterification degree (> 98%). Both highly pure FDCA and high esterification degree allowed us to reach the high molecular weight. Using the same monomer and reaction conditions, PBSF40-60 with very high M_w (162,000–167,000 g/mol) were also synthesized in our very recent reports [16,17]. The higher molecular weight resulted in some difference in thermal transition and mechanical properties, which will be discussed in the next sections. The copolymer composition of PBSF10, namely, the percentage of butylene furandicarboxylate (BF) unit, was determined from the ^{1}H NMR data, as previously reported [12,16]. It was 10.2 mol%.

3.2. Crystal structure

It was interesting to study the influence of the existence of BF unit on the crystal structure of PBSF10. The crystal structure of PBS and PBSF10 was investigated with wide angle X-ray diffraction (WAXD). Fig. 1 shows the WAXD pattern of PBS and PBSF10 samples sufficiently annealed at 95 °C. Both samples show typical profiles of semicrystalline polymers, presenting evident reflection characteristic of crystalline region, which are superimposed over bell-shape baseline due to the presence of amorphous region. It is known that PBS forms a monoclinic crystal lattice with crystal cell parameters: a = 0.523 nm, b = 0.908 nm, c = 1.079 nm, and β = 123.87° [29]. PBS shows intense diffraction peaks at 20.2°, 22.5°, 23.1° and less intense reflection at 29.5°, which are ascribed to the (0 2 0), (0 2 1), (1 1 0) and (1 1 1) planes [29]. Almost the same diffraction peaks appeared at the same position for PBSF10,

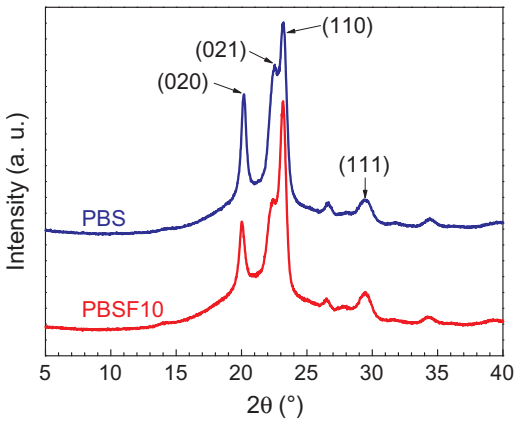

Fig. 1. WAXD patterns of PBS and PBSF10.

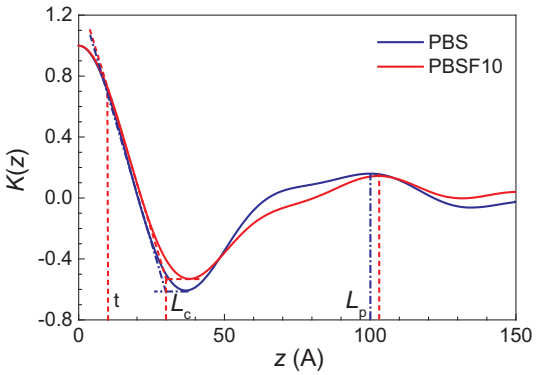

Fig. 2. One dimensional correlation function analysis of SAXD data of PBS and PBSF10 annealed at 95 °C. L_p: crystal long period; L_c: thickness of the crystalline region; t: thickness of the transition zone.

indicating that PBSF10 has the same crystal structure of PBS. Therefore, it can be concluded that the small amount of BF unit in PBSF10 is completely excluded from the PBS crystalline phase and locates at the amorphous phase. The WAXD patterns were analyzed by peak-fitting and the ratio of the total area of all crystalline reflexes to that of all reflexes was defined as the crystallinity. The crystallinities of PBS and PBSF10 are 46% and 39%, respectively.

To better understanding the difference in crystal structure between PBS and PBSF10, they are further characterized with small angle X-ray scattering (SAXS). The normalized one-dimensional correlation function (1DCF), $K(z)$, is correlated with the scattering intensity $I(q)$ with Eq. (1), in which q is the scattering vector and equal to $4\pi\sin\theta/\lambda$ (λ is the scattering wave length) and z is the spatial coordinate along the normal direction of lamella. The 1DCF analysis results of the SAXS data were obtained using the Mathematica 9.0 software and shown in Fig. 2. The crystal structure parameters including lamella long period (L_p), thickness of the crystalline region (L_c) and thickness of the transition zone (t) were obtained from the figure through a so-called graphing method. The thickness of the amorphous region (L_a) was calculated from Eq. (2). The results are listed in Table 2. It can be seen that PBS and PBSF have the same thicknesses of crystalline region and transition zone (3 nm and 1 nm), but PBSF10 has larger thickness of amorphous region than PBS (6.3 nm vs. 6.0 nm). Therefore, PBSF10 has a larger long period than PBS (10.3 nm vs. 10.0 nm). This result validated that the BF unit is excluded from the PBS crystalline phase and locates at the amorphous phase, and therefore, accounted for the less crystallinity of PBSF10. In conclusion, incorporating 10 mol% BF unit into PBS chain did not change the crystal structure of PBSF10 but thickened the amorphous region of the lamella.

$$K(z) = \frac{\int_0^\infty q^2 I(q)\cos(qz)dq}{\int_0^\infty q^2 I(q)dq} K(z) \tag{1}$$

$$L_a = L_p - L_c - t \tag{2}$$

3.3. Nonisothermal crystallization and melting behavior

The nonisothermal melt crystallization and followed melting behavior were studied with DSC. The thermograms of PBS and PBSF10 are shown in Fig. 3. In comparison with PBS, PBSF10 showed decreasing crystallization and melting temperature (T_c, T_m) and enthalpy (ΔH_c, ΔH_m), but they still retained high enough crystallizability and showed higher glass transition temperature (T_g). The T_c, T_m, ΔH_c and ΔH_m of PBSF10 decreased by 29.2 °C, 12.3 °C, 15.0 J/g, 15.5 J/g, respectively, but the T_g increased by 8.5 °C. The decrease in crystallizability is in accordance with the WAXD results. As the molecular weight of both PBS and PBSF10 was higher than those in our previous study [12], their crystallizability decreased and therefore, their T_c, T_m, ΔH_c and ΔH_m decreased accordingly, as shown in Table 1. On the other hand, PBSF10 has clearly higher thermal transition properties than PBSF45 (T_m: 101.6 °C vs 73.1 °C [16]; ΔH_m: 49.6 J/g vs. 18.4 J/g [16]) which has the same aromatic content as in commercialized PBAT.

Table 2
Crystal structure and thermal transition parameters of PBS and PBSF10.

Sample	L_p (Å)	L_c (Å)	t (Å)	L_a (Å)	T_g (°C)	T_c (°C)	T_m (°C)	ΔH_c (J/g)	ΔH_m (J/g)	Ref.
PBS	100	30	10	60	−36.1	68.5	113.9	62.3	64.6	This study
PBSF10	103	30	10	63	−27.6	39.3	102.0	46.8	49.6	This study
PBS*	–	–	–	–	−40.0	76.6	114.0	75.9	74.8	[12]
PBSF10*	–	–	–	–	−25.0	53.1	104.0	65.2	61.9	[12]

L_p: crystal long period; L_c: thickness of the crystalline region; t: thickness of the transition zone; L_a: thickness of the amorphous region.

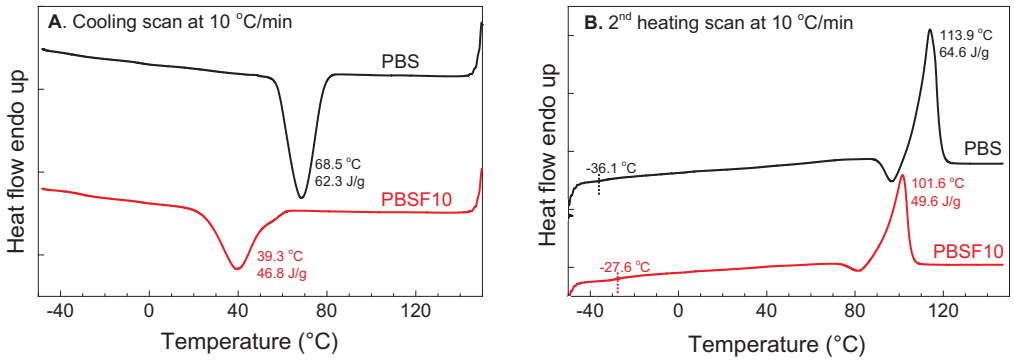

Fig. 3. DSC curves of PBS and PBSF10 copolyester.

3.4. Isothermal crystallization and melting behavior

The isothermal melt crystallization of PBSF10 was conducted at crystallization temperature (T_c) ranging 57.5–82.5 °C, higher than the nonisothermal melt crystallization peak temperature (39.3 °C, seen Fig. 3). The Avrami plots of relative crystallinity versus crystallization time are shown in Fig. 4. It can be seen that the crystallization kinetics was well described by Avrami equation (Eq. (3)). The Avrami index n varied in the range 2.10–2.87. The half crystallization time ($t_{1/2}$) was calculated with Eq. (4) from the crystallization rate constant k. It is found that the total crystallization rate ($t_{1/2}{}^{-1}$) decreased exponentially with increasing isothermal crystallization temperature in the experimental range, as shown in Fig. 5. The resulting empirical relationship between $t_{1/2}{}^{-1}$ and T_c is described in Eq. (5). The $t_{1/2}$ value was 0.87 min at 57.5 °C, indicating high crystallization rate.

$$\log[-\ln(1-X_t)] = \log k + n\log t \tag{3}$$

$$t_{1/2} = (\ln 2/k)^{1/n} \tag{4}$$

$$\ln(t_{1/2}^{-1}) = 8.93-0.152T_c \tag{5}$$

After isothermal melt crystallization, the samples were heated at 10 °C/min to 150 °C to observe the melting behavior. In the heating scan (Fig. 6A), all samples exhibited three endothermal melting peaks, denoted as peaks I, II and III. With increasing T_c, peak I kept very weak, peak II broadened and moved to higher temperature, and peak III diminished and shifted slightly toward higher temperature. The peaks II and III tended to merge at high T_c. Similar multiple melting peaks were also observed in PBS [30,31] and some other polyesters [32]. Peak I is ascribed to melting of small and imperfect secondary crystals, peak II is attributed to melting of primary crystals formed during the crystallization at T_c, and peak III is ascribed to melting of recrystallized ones. When the corresponding peak temperatures ($T_{m,I}$, $T_{m,II}$, $T_{m,III}$) were plotted versus T_c (Fig. 6B), it can be seen that all of them raise with T_c linearly in the experimental range, $T_{m,I}$ keeps about 5.2 °C higher than T_c, and the slope decreases in such an order $T_{m,I} > T_{m,II} > T_{m,III}$. The less pronounced T_c dependence of $T_{m,III}$ indicates peak III relates to more perfect crystals [33]. According to the well-known Hoffman-Week's equation ($T_m = T_m{}^0(1–1/(2\beta)) + T_c/(2\beta)$, in which β is the ratio of the thickness of the final crystallites L_c to that of the preliminary ones $L_c{}^*$) [34], the equilibrium melting point ($T_m{}^0$) can be obtained as the intercept of the $T_{m,II}$-T_c line with the diagonal line ($T_m = T_c$). The $T_m{}^0$ of PBSF10 was estimated to be 122 °C. It is 15.5 °C lower than that of PBS (137.5 °C, 136.3 °C) [30,31].

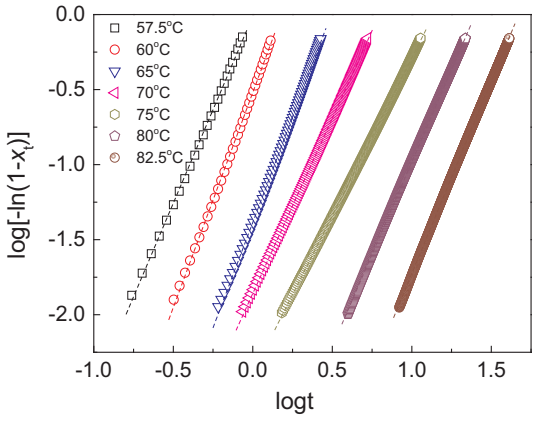

Fig. 4. Avrami fitting of the isothermal melt crystallization of PBSF10.

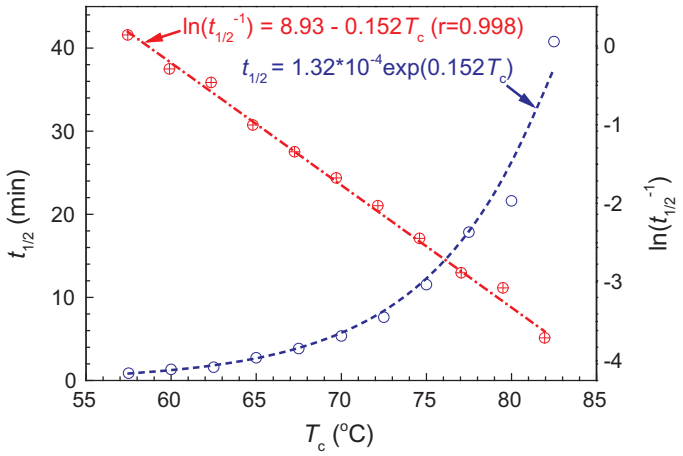

Fig. 5. T_c dependence of the half crystallization time $t_{1/2}$ of PBSF10.

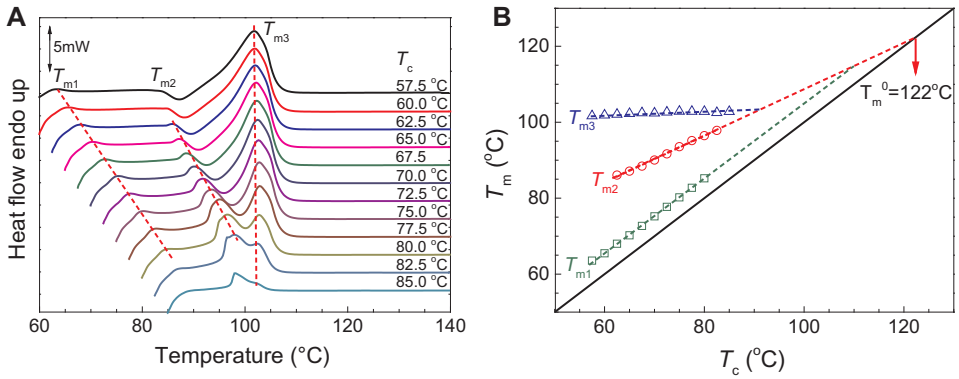

Fig. 6. (A) Heating scan (10 °C/min) DSC curves after isothermal melt crystallization at the indicated temperature and (B) Hoffman-Weeks plot of PSF10.

3.5. Spherulite growth kinetics

The spherulite growth of PBSF10 was observed by POM in the T_c range of 70–90 °C. It was seen from the POM micrographs (not shown) that the spherulite density decreased with increasing T_c. The spherulite size grew linearly with time until the spherulites contacted with each other. The spherulite growth rate (G) was calculated as the slope of spherulite radius-time curve. The T_c dependence of the spherulite growth rate is visualized in Fig. 7. Clearly, the growth rate decreased with increasing T_c from 70 °C to 90 °C because the supercooling degree, namely the thermodynamic driving force for spherulite growth, decreased accordingly.

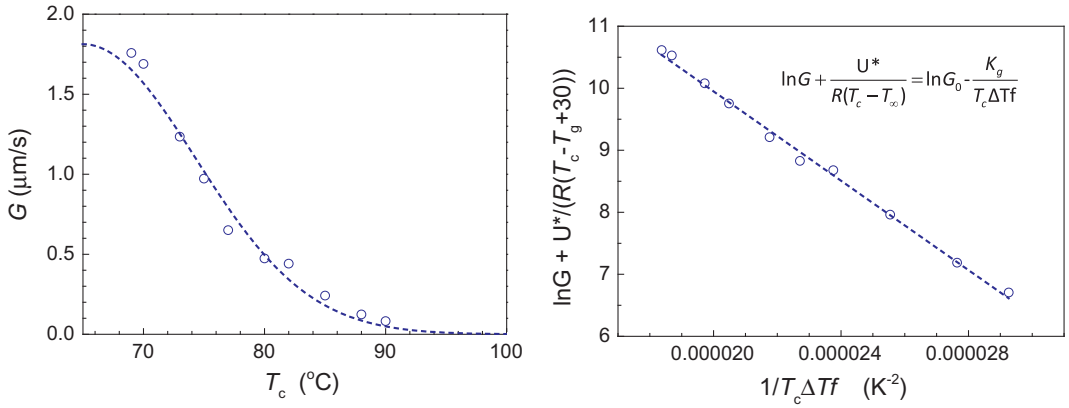

Fig. 7. (A) Growth of spherulite size with crystallization time at various temperature and (B) spherulite size growth rate of PBSF10 at various crystallization temperatures.

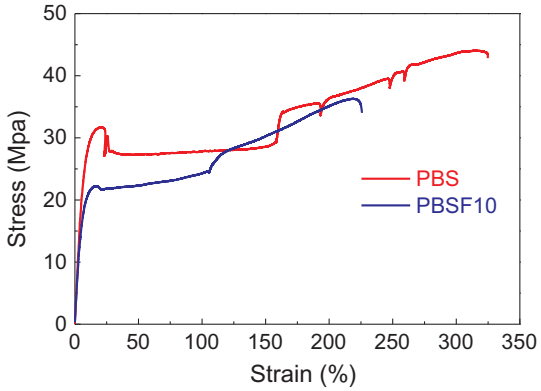

Fig. 8. Tensile stress-strain curves of PBS and PBSF10.

The T_c dependence of spherulitic growth rate of PBSF10 was further analyzed with Lauritzen-Hoffman equation (Eq. (6)), where G_0 is a pre-exponential factor, U^* is the transport activation energy, T_∞ is a hypothetical temperature below which all viscous flow ceases, K_g is a nucleation parameter, ΔT is the supercooling degree, and f is a correction factor to account for the variation in the bulk enthalpy of fusion per unit volume with temperature, $f = 2T_c/({T_m}^0 + T_c)$. The universal values of $U^* = 1500$ cal/mol and $T_\infty = T_g - 30$ K were used in the calculation and the results are plotted in Fig. 7B. Quite good linear relationship was observed and no regime transition appeared in the experimental T_c range. The slope of the curve gives a high value of K_g, $3.60 * 10^5$ K^2.

$$\ln G + \frac{U^*}{R(T_c - T_\infty)} = \ln G_0 - \frac{K_g}{T_c \Delta T f} \tag{6}$$

3.6. Tensile properties

Finally, the tensile properties of PBS and PBSF10 were also assessed and compared. As they are flexible crystalline plastics, elastic deformation followed by yielding and strain hardening were observed in stress-strain curves (Fig. 8). The tensile properties are listed in Table 3. Both of them have satisfactory tensile properties: modulus 370–430 MPa, strength at break 38–44 MPa and elongation at break 230–300%. In comparison with PBS, PBSF10 has lower tensile properties because of its lower extent of crystallinity. In comparison with our previous results, the PBS and PBSF10 samples in this study exhibited lower modulus but higher tensile strength and elongation at break because of their higher molecular weight and lower crystallinity. In comparison with PBSF45 which also has very high M_w [16], the PBSF10 has much higher tensile modulus (372 MPa vs. 64 MPa), as seen in Table 3. The PBSF10 sample also shows higher tensile strength and modulus when compared with poly(butylene succinate-co-adipate) and poly(butylene succinate-co-terephthalate) with the same composition (PBSA10, PBST10) reported in literatures [23,26]. Besides, the T_g of PBSF10 is higher than that of PBSA10 and PBST10 (−27.6 °C vs. −39 °C [27], −37 °C [23]) though they have almost the same T_m (103 ± 2 °C [23,26–27]).

4. Conclusions

In this study, high molecular weight PBSF10 was synthesized and its crystal structure, crystallization-melting behavior and tensile properties were investigated. In comparison with PBS, PBSF10 has the same crystal structure with the same thicknesses of crystalline region and transition zone (3 nm and 1 nm), but larger thickness of amorphous region (6.3 nm vs. 6.0 nm), indicating that the BF unit is excluded from the crystalline region and located in the amorphous region. Therefore, PBSF10 exhibits less crystallizability than

Table 3
Tensile properties of PBS, PBSF10, PBSA10 and PBST10.

Sample	M_w (g/mol)	T_m (°C)	ΔH_m (J/g)	E (MPa)	σ_b (MPa)	ε_b (%)	Reference
PBS	162,500	113.9	64.6	432 ± 22	43.6 ± 1.0	303 ± 15	This study
PBSF10	193,700	102.0	49.6	372 ± 20	38.0 ± 3.0	228 ± 6	This study
PBS*	35,100	114.0	74.8	675 ± 5	30.6 ± 1.4	128 ± 14	Ref. [12]
PBSF10*	55,800	104.0	61.9	554 ± 30	21.4 ± 3.4	165 ± 41	Ref. [12]
PBSF45	165,400	73.1	18.4	64 ± 1	56 ± 3	758 ± 17	Ref. [16]
PBST10[a]	–	103	62	331	22	415	Ref. [23]
PBSA10[b]	–	105	59	–	18.3	402	Ref. [26]

[a] PBST10 is poly(butylene succinate-co-terephthalate) with 10 mol% butylene terephthalate unit.
[b] PBSA10 is poly(butylene succinate-co-adipate) with 10 mol% butylene adipate unit. The tensile properties of PBSA10 are obtained by interpolation method from the data of PBS and PBSF10 reported in Ref. [26].

PBS. But PBSF10 still exhibits rapid nonisothermal and isothermal crystallization. The half crystallization time was low as 0.9 min at 57.5 °C, and the nucleation parameter is as high as $3.60 * 10^5$ K^2. The equilibrium melting temperature is estimated to be 122 °C. Because of high molecular weight and good crystallizability, the PBSF10 sample exhibited good tensile properties: modulus 370 MPa, strength at break 38 MPa and elongation at break 230%.

Acknowledgements

The authors thank the National Nature Science Foundation of China (No. 51373152), the National Key Research and Development Program (2016YFB0302402) and 151 Talents Project of Zhejiang Province for financial support.

References

[1] J.A. Galbis, M.G. García-Martín, M.V. de Paz, E. Galbis, Synthetic polymers from sugar-based monomers, Chem. Rev. 116 (2016) 1600–1636.
[2] S.A. Miller, Sustainable polymers: replacing polymers derived from fossil fuels, Polym. Chem. 5 (2014) 3117–3118.
[3] W. Amass, A. Amass, B. Tighe, A review of biodegradable polymers: uses, current developments in the synthesis and characterization of biodegradable polyesters, blends of biodegradable polymers and recent advances in biodegradation studies, Polym. Int. 47 (1998) 89–144.
[4] R. Auras, B. Harte, S. Selke, An overview of polylactides as packaging materials, Macromol. Biosci. 4 (2004) 835–864.
[5] A. Sodergard, M. Stolt, Properties of lactic acid based polymers and their correlation with composition, Prog. Polym. Sci. 27 (2002) 1123–1163.
[6] R.J. Müller, U. Witt, E. Rantze, W.D. Deckwer, Architecture of biodegradable copolyesters containing aromatic constituents, Polym. Degrad. Stab. 59 (1998) 203–208.
[7] U. Witt, M. Yamamoto, U. Seeliger, R.J. Müller, V. Warzelhan, Biodegradable polymeric materials – not the origin but the chemical structure determines biodegradability, Angew. Chem. Int. Ed. 38 (1999) 1438–1442.
[8] Z.H. Gan, K. Kuwabara, M. Yamamoto, H. Abe, Y. Doi, Solid-state structures and thermal properties of aliphatic–aromatic poly(butylene adipate-co-butylene terephthalate) copolyesters, Polym. Degrad. Stab. 83 (2004) 289–300.
[9] K.O. Siegenthaler, A. Künkel, G. Skupin, M. Yamamoto, Ecoflex® and Ecovio®: biodegradable, performance-enabling plastics, in: B. Rieger, A. Künkel, W.G. Coates, R. Reichardt, E. Dinjus, A.T. Zevaco (Eds.), Synthetic Biodegradable Polymers, Springer, Berlin, Heidelberg, 2012, pp. 91–136.
[10] T. Werpy, G. Petersen (Eds.), Top Value Added Chemicals from Biomass, vol. 1, United States Department of Energy, Washington DC, 2004, pp. 21–64 (Chapter 9).
[11] V. Mittal (Ed.), Renewable Polymers: Synthesis, Processing, and Technology, John Wiley and Sons, 2011.
[12] L.B. Wu, R. Mincheva, Y.T. Xu, J.M. Raquez, P. Dubois, High molecular weight poly(butylene succinate-co-butylenefurandicarboxylate) copolyesters: from catalyzed polycondensation reaction to thermomechanical properties, Biomaromolecules 13 (2012) 2973–2981.
[13] N. Jacquel, R. Saint-Loup, J.P. Pascault, A. Rousseau, F. Fenouillot, Bio-based alternatives in the synthesis of aliphatic-aromatic polyesters dedicated to biodegradable film applications, Polymer 59 (2015) 234–242.
[14] W.D. Zhou, X. Wang, B. Yang, Y. Xu, W. Zhang, Y. Zhang, J. Ji, Synthesis, physical properties and enzymatic degradation of bio-based poly(butylene adipate-co-butylene furandicarboxylate) copolyesters, Polym. Degrad. Stab. 98 (2013) 2177–2183.
[15] B.S. Wu, Y.T. Xu, Z.Y. Bu, L.B. Wu, B.G. Li, P. Dubois, Biobased poly(butylene 2,5-furandicarboxylate) and poly(butylene adipate-co-butylene 2,5-furandicarboxylate)s: from synthesis using highly purified 2,5-furandicarboxylic acid to thermo-mechanical properties, Polymer 55 (2014) 3648–3655.
[16] S.B. Peng, B.S. Wu, L.B. Wu, B.G. Li, P. Dubois, Hydrolytic degradation of biobased poly(butylene succinate-cofurandicarboxylate) and poly(butylene adipate-co-furandicarboxylate) copolyesters under mild conditions, J. Appl. Polym. Sci. 134 (2017) 44674.
[17] S.B. Peng, L.B. Wu, B.G. Li, P. Dubois, Hydrolytic and compost degradation of biobased PBSF and PBAF copolyesters with 40–60 mol% BF unit, Polym. Degrad. Stab. (2017), http://dx.doi.org/10.1016/j.polymdegradstab.2017.07.016.
[18] M. Soccio, M. Costa, N. Lotti, M. Gazzano, V. Siracusa, E. Salatelli, P. Manaresi, A. Munari, Euro. Polym. J. 81 (2016) 397–412.
[19] A. Terzopoulou, V. Tsanaktsis, D.N. Bikiaris, S. Exarhopoulos, D.G. Papageorgioud, G.Z. Papageorgiou, Biobased poly(ethylene furandicarboxylate-co-ethylene succinate) copolyesters: solid state structure, melting point depression and biodegradability, RSC Adv. 6 (2016) 84003–84015.
[20] Z.L. Yu, J.D. Zhou, F. Cao, B.B. Wen, X. Zhu, P. Wei, Chemosynthesis and characterization of fully biomass-based copolymers of ethylene glycol, 2,5-furandicarboxylic acid, and succinic acid, J. Appl. Polym. Sci. 130 (2013) 1415–1420.
[21] H.C. Ki, O.O. Park, Synthesis, characterization and biodegradability of the biodegradable aliphatic-aromatic random copolyesters, Polymer 42 (2001) 1849–1861.
[22] S.L. Luo, F.X. Li, J.Y. Yu, A.M. Cao, Synthesis of poly(butylene succinate-co-butylene terephthalate) (PBST) copolyesters with high molecular weights via direct esterification and polycondensation, J. Appl. Polym. Sci. 115 (2010) 2203–2211.
[23] M. Nagata, H. Goto, W. Sakai, N. Tsutsumi, Synthesis and enzymatic degradation of poly(tetramethylene succinate) copolymers with terephthalic acid, Polymer 41 (2000) 4373–4376.
[24] Y.J. Sun, L.B. Wu, Z.Y. Bu, B.G. Li, N.X. Li, J.M. Dai, Synthesis and thermomechanical and rheological properties of biodegradable long-chain branched poly (butylene succinate-cobutylene terephthalate) copolyesters, Ind. Eng. Chem. Res. 53 (2014) 10380–10386.
[25] J. Lu, L.B. Wu, B.G. Li, Long chain branched poly(butylene succinate-co-terephthalate) copolyesters using pentaerythritol as branching agent: synthesis, thermo-mechanical, and rheological properties, J. Appl. Polym. Sci. 133 (2016) 44544.
[26] V. Tserki, P. Matzinos, E. Pavlidou, D. Vachliotis, C. Panayiotou, Biodegradable aliphatic polyesters. Part I. Properties and biodegradation of poly(butylene succinate-co-butylene adipate), Polym. Degrad. Stab. 91 (2016) 367–376.
[27] R.A. Pérez-Camargo, B. Fernández-d'Arlas, D. Cavallo, T. Debuissy, E. Pollet, L. Avérous, A.J. Müller, Tailoring the structure, morphology, and crystallization of isodimorphic poly(butylene succinate-ran-butylene adipate) random copolymers by changing composition and thermal history, Macromolecules 50 (2017) 597–608.
[28] F.W. Billmeyer, Methods for estimating intrinsic viscosity, J. Polym. Sci. 4 (1949) 83–86.
[29] K.J. Ihn, E.S. Yoo, S.S. Im, Structure and morphology of poly(tetramethylene succinate) crystals, Macromolecules 28 (1995) 2460–2464.
[30] Z.B. Qiu, T. Ikehara, T. Nishi, Miscibility and crystallization in crystalline/crystalline blends of poly(butylene succinate)/poly(ethylene oxide), Polymer 44 (2003) 2799–2806.
[31] G.Y. Wang, Z.B. Qiu, Synthesis, crystallization kinetics, and morphology of novel biodegradable poly(butylene succinate-co-hexamethylene succinate) copolyesters, Ind. Eng. Chem. Res. 51 (2012) 16369–16376.
[32] G. Stoclet, G.G. du Sart, B. Yeniad, S. de Vos, J.M. Lefèbvre, Isothermal crystallization and structural characterization of poly(ethylene-2,5-furandicarboxylate), Polymer 72 (2015) 165–176.
[33] G.Z. Papageorgiou, V. Tsanaktsis, D.N. Bikiaris, Synthesis of poly(ethylene furandicarboxylate) polyester using monomers derived from renewable resources: thermal behavior comparison with PET and PEN, Phys. Chem. Chem. Phys. 16 (2014) 7946–7958.
[34] J. Hoffman, J.J. Weeks, Melting process and equilibrium melting temperature of polychlorotrifluoroethylene, J. Res. Natl. Bur. Stand. 66A (1962) 13–28.